The Cerebellum (2019) 18:536–543
https://doi.org/10.1007/s12311-019-01026-4

ORIGINAL PAPER

# Human Brain Region-Specific Alternative Splicing of TRPC3, the Type 3 Canonical Transient Receptor Potential Non-Selective Cation Channel

Jennie M. E. Cederholm[1] · Youngsoo Kim[1] · Georg von Jonquieres[1] · Gary D. Housley[1]

Published online: 18 March 2019


## Abstract

Canonical transient receptor potential (TRPC) non-selective cation channels are broadly expressed by neurons, glia and the microvasculature of the brain. In neurons and astrocytes, these ion channels are coupled to group I metabotropic glutamate receptors via Gαq–phospholipase C signal transduction. In the mouse cerebellar Purkinje neurons, TRPC channels assembled as tetramers of TRPC3 subunits exclusively mediate this glutamatergic signalling mechanism and regulation of alternative splicing results in dominance of a high $Ca^{2+}$ conducting TRPC3c isoform. This regional control of *TRPC3* transcript type likely has physiological and pathophysiological sequelae. The current study provides a quantitative comparison of the *TRPC3c* splice variant and the *TRPC3b* full-length isoform expression across seven regions of the human brain. This shows that the cerebellum has the highest expression level of both isoforms and that regulation of alternative splicing results in a higher propensity of the TRPC3c isoform in the cerebellum relative to the TRPC3b isoform (in a 1:3 ratio). This compares with the other regions (motor cortex, hippocampus, midbrain subregions, pons and medulla) where the prevalence of *TRPC3c* relative to *TRPC3b* is typically less than half as abundant. The finding here of a bias in the high-conductance TRPC3c isoform in the cerebellum is consistent with the enhanced vulnerability of the cerebellum to ischaemic injury.

**Keywords** mGluR-coupled cation channel · TRPC3 CIRB domain · Cerebellum · Hind- and midbrain · Hippocampus · Cortex

## Introduction

Canonical transient receptor potential channel type 3 (TRPC3) subunits undergo homo- or heteromeric assembly to form tetrameric non-selective cation channels with broad expression throughout the brain [1, 2]. TRPC3 is particularly prominent in the cerebellar cortex across species including human [3–6]. The TRPC3 channel is known for its multi-modal activation mechanism. The channel is activated by the Gαq protein-coupled receptor–phospholipase C–diacylglycerol pathway [7, 8]. In mouse cerebellar Purkinje neurons, TRPC3 has been shown to be exclusively coupled to the class I metabotropic receptor mGluR1 to support the slow excitatory post-synaptic current (sEPSC) evident with stimulation of the parallel fibre input [3]. TRPC3 channels have also been shown to be positively modulated by depletion of intracellular $Ca^{2+}$ stores [9, 10]. The TRPC3 channel interacts with STIM1, which is an endoplasmic reticulum $Ca^{2+}$ sensor. This interaction is achieved through hetero-oligomerization with TRPC1 [11, 12].

The TRPC3 channel has several important regulatory domains. Notably, the C-terminal tail contains a segment known as the calmodulin–inositol trisphosphate receptor (CaM–$IP_3R$) binding domain (CIRB). This is encoded by exons 9 and 10 [13]. A study of the interaction of CaM and $IP_3R$ peptides with recombinant TRPC3 showed that both competitively bind to the TRPC3 CIRB domain to regulate the channel activity [13]. Rises in $[Ca^{2+}]_i$ drive $Ca^{2+}$–CaM complex binding to the CIRB domain, leading to inhibition of channel opening. Conversely, low $[Ca^{2+}]_i$ reduce this inhibitory $Ca^{2+}$–CaM binding, and promotion of binding of $IP_3R$, leading to increase channel opening. The CIRB domain has also been suggested to affect membrane expression, with recombinant

**Electronic supplementary material** The online version of this article (https://doi.org/10.1007/s12311-019-01026-4) contains supplementary material, which is available to authorized users.

✉ Gary D. Housley
g.housley@unsw.edu.au

[1] Translational Neuroscience Facility and Department of Physiology, School of Medical Sciences, The University of New South Wales, Sydney, New South Wales 2052, Australia

TRPC3 protein chimaeras lacking the CIRB motif failing to be expressed on the plasma membrane [10].

We have previously identified an alternative splice variant of *TRPC3*, designated TRPC3c protein across mouse, rat and guinea pig [14]. We subsequently isolated the mRNA for the *TRPC3c* splice variant from human cerebellum (accession number KC207570.1) [15]. The *TRPC3c* mRNA transcript lacks exon 9, which codes for the proximal part of the CIRB domain, associated with the $IP_3R$ binding site (see Supplementary Fig. 1). Using heterologous expression in human embryonic kidney HEK293 cells, the TRPC3c channels exhibited higher channel opening frequency compared to the TRPC3b isoform, driving significantly greater $Ca^{2+}$ entry when activated via the endogenous M3 muscarinic acetylcholine receptor, or via recombinant mGluR1 receptors [14]. Given the wide expression of TRPC3 in the brain, and the coupling of this ion channel to the class I mGluR [3], TRPC3-mediated cation flux and $Ca^{2+}$ entry are likely to be prominent modulators of neuronal function, and in the case of sustained mGluR activation, which occurs with stroke, traumatic brain injury and epilepsy, the ion conductance profile of TRPC3c in particular is likely to be a prominent contributor to pathophysiology.

The balance of expression of TRPC3c to TRPC3b is therefore of particular significance with respect to potential variation in vulnerability of different regions of the brain. Semi-quantitative studies of *TRPC3c* and *TRPC3b* mRNA expression based on end-point RT-PCR demonstrated region-specific regulation of this alternative splicing in mouse, rat and guinea pig, with *TRPC3c* being dominant in the cerebellum compared with *TRPC3b* dominance in other brain regions. A head-to-head comparison of vulnerability to focal ischaemic brain injury in mouse demonstrated that the cerebellum was significantly more vulnerable than the cerebral cortex, which may be attributed to the regional dominance of this TRPC3c isoform in the cerebellum [16]. It is therefore of particular clinical relevance to consider the relative expression of TRPC3c against TRPC3b in different regions of the human brain. This was addressed in the current study by using quantitative SYBR® green-based qRT-PCR analysis of these two mRNA transcripts in human brain tissue blocks across seven regions. The data indicate that, as in the rodent and guinea pig models, human *TRPC3* mRNA splice variants are regulated in a region-specific manner.

## Materials and Methods

### Human Subjects

Human brain tissue from males and females (52–103 years old) (Supplementary Table 1) was received from the Sydney Brain Bank (Neuroscience Research Australia; 3 subjects) and the New South Wales (NSW) Tissue Resources Centre (Department of Pathology, University of Sydney; 7 subjects). Both brain tissue centres have approvals from relevant human research ethics committees, and tissue requests are reviewed and approved by the NSW Brain Banks Scientific Review Committee or the National Institutes of Health (NIAAA) Scientific Advisory Board. The study was approved by the UNSW Sydney Human Research Ethics Committee. Brain regions studied were the motor cortex, hippocampus, inferior and superior midbrain, pons, medulla and cerebellum.

### RNA Extraction and Generation of cDNA

Total RNA extraction was performed from seven brain regions of the subjects using an RNeasy Mini kit (Qiagen, The Netherlands) according to the manufacturer's instructions. Each sample (approximately 30 mg in weight) was homogenised in 600 μl of buffer RLT containing 1% of β-mercaptoethanol (Sigma-Aldrich, USA). The homogenate was transferred to a gDNA eliminator spin column to remove genomic DNA. After being centrifuged at 10,000×*g* for 30 s, the flow-through mixture was added with 600 μl of 70% ethanol. The mixture was then transferred to a RNeasy spin column and centrifuged at 10,000×*g* for 15 s to trap the RNA in the cellulose resin. This was followed by a DNase treatment step, where 10 μl of DNase I (3 units/μl, Qiagen, USA) and 70 μl of buffer RDD were added to the cellulose resin containing the RNA. Following incubation for 15 min at room temperature, the resin was washed with 350 μl of buffer RW1. The resin was then washed with 500 μl of buffer RPE twice, and the RNA was collected in 50 μl of $dH_2O$. The RNA was diluted to a concentration of 25 ng/μl, with a typical sample yield of ~ 350 ng. Samples that could not meet this concentration due to poor yield were discarded. The final sample numbers for the different brain regions were the following: motor cortex, $n = 6$; hippocampus, $n = 7$; midbrain superior, $n = 2$; midbrain inferior, $n = 5$; pons, $n = 6$; medulla, $n = 3$; cerebellum, $n = 8$. These samples were reverse transcribed using random hexamer primers from a high-capacity cDNA reverse transcription kit (Applied Biosystems, U.S.A.) according to the manufacturer's instructions. The reaction mix was prepared for each RNA sample. The reaction mix consisted of 10 μl of total RNA, along with the following reagents available in the kit: 2 μl of 2× reverse transcription buffer, 0.8 μl of dNTP mix (100 mM), 1 μl of random primers, 1 μl of MultiScribe™ reverse transcriptase (50 units/μl), 1 μl of RNase inhibitor and 3.2 μl of $H_2O$. The reaction was then performed in Epgradient S thermal cycler (Eppendorf, Germany) with the following steps: primer binding at 25 °C for 10 min, DNA synthesis at 37 °C for 120 min and inactivation of the reaction at 85 °C for 5 min.

## PCR Amplicon Production of Human *TRPC3b* and *TRPC3c* Splice Variant cDNAs

The alternative splicing variant of *TRPC3*, referred to as *TRPC3c*, has previously been reported in brain tissue of mouse, rat and guinea pig [14], where a dominant expression of *TRPC3c* was found in the cerebellum compared to other brain regions. We have also isolated the mRNA for this splice variant from human cerebellum [15] (Accession number KC207570.1). In the current study, *TRPC3b* and the *TRPC3c* splice variant PCR amplicons were produced using primers that targeted the coding regions of exons 8 and 10. Use of a forward primer (nucleotides 2224–2241) and reverse primer (nucleotides 2372–2354) generated a 149 bp *TRPC3b* amplicon and a 65 bp *TRPC3c* amplicon (Fig. 1), subsequently validated by sequencing. The thermal cycle profile for the PCR (40 cycles) was denaturation at 95 °C for 30 s, annealing at 58 °C for 30 s and extension at 72 °C for 60 s.

## Generation of cDNA Templates for qRT-PCR Standard Curve Analysis

Full length *TRPC3b* and *TRPC3c* cDNA templates for the standard curves were custom-made by Epoch Life Science (Texas, USA; *TRPC3b*, 3306 bp; *TRPC3c*, 3305 bp), while the *β-ACTIN* (gene code *ACTB*) and *glyceraldehyde-3-phosphate dehydrogenase* (*GAPDH*) cDNA templates were made in-house using conventional PCR to produce larger amplicons flanking the qRT-PCR targets (Table 1; primer design). The reaction mixture (25 μl) contained 2 μl of sample cDNA (human cerebellum cDNA, 1:10 dilution), 10 μM of each primer, 10 mM dNTPs, 10× buffer and TaqDNA polymerase. The PCR profile (35 cycles) was denaturation at 95 °C for 30 s, annealing at 58 °C for 30 s and extension at 72 °C for 60 s. The *β-ACTIN* and *GAPDH* PCR products generated in this way were purified by ethanol precipitation as follows: 1/10 of the total sample volume of NaAc (5 mM, pH 5.2) was added followed by 300 μl of 100% ethanol. Samples were mixed and left on ice for 10 min before being centrifuged for 10 min (13,000×*g*). The supernatant was then removed, pellet was washed using 500 μl of 70% ethanol and centrifuged again for 5 min (13,000×*g*). The pellet was allowed to air dry before being resuspended in 100 μl TE buffer (10 mM TRIS HCl, 1 mM EDTA). The DNA concentration (ng/μl) of each of the four templates was determined by UV spectroscopy (NanoDrop® ND-1000, Thermo Scientific), and the copy number was calculated using the ENDMEMO copy number calculator (http://endmemo.com/bio/dnacopynum.php). From this, stock templates were diluted to a copy number of $1 \times 10^{10}$ molecules/μl, and then serially diluted to generate the cDNA for the standard curves. Standard curves were automatically generated by the StepOnePlus real-time PCR system by plotting cycle threshold ($C_t$) against copy number (using a $10^3$ to $10^7$ standard dilution series).

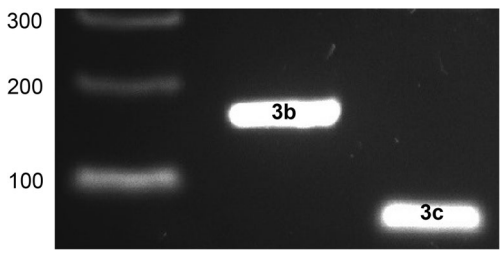


**Fig. 1** Agarose gel electrophoresis showing *TRPC3b* (left 149 bp) and *TRPC3c* (right 65 bp) PCR amplicons with size determined by sequencing of the cloned cDNA. Note the difference in the size of the two isoforms, resulting from the absence of exon 9 in the *TRPC3c* splice variant

## Quantitative Real-Time PCR

Quantification of two splice variants of the human *TRPC3* (*TRPC3b* and *TRPC3c*) and two reference genes, *GAPDH* and *β-ACTIN*, was performed using gene-specific primers (Table 1; Integrated DNA Technologies, Baulkham Hills, NSW, Australia), SYBR® green (Thermo Fisher Scientific, Waltham, MA, USA) and the StepOnePlus real-time PCR system (Applied BioSystems, CA, USA). The reaction mixture (20 μl) contained 2 μl of sample cDNA (1:10 dilution), 200 nM of each primer and 2× SYBR® green master mix. The PCR protocol was heating for 10 min at 95 °C followed by 40 cycles of 15 s at 95 °C and 1 min at 58 °C. Each 96-well plate contained triplicate templates for the unknown cDNA from one tissue region of an individual against the four primer targets (*TRPC3b*, *TRPC3c*, *β-ACTIN* and *GAPDH*), along with copy number standards in triplicate for each of the primer targets. No-template controls were also included for each primer target and invariably failed to exhibit exponential growth functions of the SYBR® green fluorescent signal out to the 40-cycle limit. Cycle threshold ($C_t$) values, which represent the interpolated thermal cycle number at the inflection point for exponential PCR amplification of the templates were determined using StepOne™ software (v.2.3, Applied Biosystems; see Supplementary Fig. 2 for examples). The copy number was then calculated by the best fit to the standards by the software. This was validated by linear regression best fits of the standards (Supplementary Fig. 3 and Supplementary Table 2). The slopes of the standard curves for each of the four primer targets approached the theoretical value of − 3.32, which represents a PCR reaction where the number of template molecules double with each cycle and hence are 100% efficient [20, 21] (Supplementary Table 2).

## Statistical Analysis

To enable comparison of the expression levels for each of the *TRPC3* variants across brain regions, *TRPC3b* transcript copy

**Table 1** Primer sequences for human *TRPC3b*, *TRPC3c*, *β-ACTIN* and *GAPDH*

| Gene | GenBank accession number | Forward primer (5′–3′) | Reverse primer (5′–3′) | Modified from reference |
|---|---|---|---|---|
| For qRT-PCR reactions | | | | |
| *TRPC3b* | Y13758 | CAGCATTCTCAATCAGCCA | TAACGAAGGCTGGAGATA | Xu et al. 1997 [17] |
| *TRPC3c* | KC207570.1 | ATTACCTCCACCTTTCAG | AGTCTTTTCATTATCTGCCT | |
| *GAPDH* | NM_002046.5 | TGACAACTTTGGTATCGTGG | CACAGTCTTCTGGGTGGCAGTGAT | Greenwood et al. 2007 [18] |
| *β-ACTIN* | NM_001101 | GAGCGCGGCTACAGCTT | TCCTTAATGTCACGCACGATTT | Mori et al. 2008 [19] |
| For generation of standard curve templates | | | | |
| *GAPDH* | NM_002046.5 | CTTAGCACCCCTGGCC | CCATCACGCCACAGTTTC | Greenwood et al. 2007 [18] |
| *β-ACTIN* | NM_001101.3 | GACTGACTACCTCATGAAGATCC | CATCTCTTGCTCGAAGTCC | |

number and *TRPC3c* transcript copy number were separately normalised to two different reference genes (*β-ACTIN* and *GAPDH*). This allows for correction in tissue mass, efficiency of RNA isolation, reverse transcription efficiency for each sample and sample-to-sample variations [22]. Thus, for each cDNA template, copy number data were obtained in triplicate for each of the four primer sets to derive the average fractional copy number relative to either the *β-ACTIN* or *GAPDH* transcript copy number for each subject for that brain region. These data were analysed using a three-way ANOVA, with validation of normal distribution of the data, and ranked two-way ANOVAs for each of the *TRPC3* splice variants. In order to determine the relative expression of *TRPC3b* against *TRPC3c* for each brain tissue region, a ratiometric analysis was performed. This used the *TRPC3b* and *TRPC3c* data from the reference gene normalised data set, augmented with two additional PCR replicates per target from each tissue cDNA template pool (a total of 5 replicates each, per sample). This yielded data on the relative expression level of *TRPC3c* compared to *TRPC3b* irrespective of the absolute expression level in a brain region. For each brain region, a one sample *t* test (ranked values for motor cortex, midbrain inferior and pons) was used to test variance from a mean predicted ratio value of 1 (equal expression). Overall comparison of proportions across brain regions was undertaken using a ranked two-way ANOVA.

## Results

### Quantitative Comparison of *TRPC3b* and *TRPC3c* Normalised Against Reference Genes

The variation in expression of the two *TRPC3* splice variants across seven brain regions was studied using *TRPC3b* and *TRPC3c* transcript levels normalised to each of two reference genes (*β-ACTIN* and *GAPDH*) known to be broadly expressed across cell types at high copy number [23]. This provided independence from variations in tissue sample mass and mRNA quality. The mean mRNA transcript copy numbers for individual subjects across the four gene targets are provided in Supplementary Tables 3, 4, 5, and 6, with the data from Tables 3 and 4 (*TRPC3b* and *TRPC3c*), respectively, plotted in Supplementary Fig. 4. A three-way ANOVA analysis indicated that the data on *TRPC3b* and *TRPC3c* copy number normalised to either of the reference genes were indistinguishable ($p = 0.172$); the transcript numbers of *β-ACTIN* and *GAPDH* were comparable within the brain regions studied (Supplementary Fig. 5). Overall, *TRPC3b* expression was significantly greater than *TRPC3c* ($p < 0.001$). Associated ranked two-way ANOVA with Holm–Sidak multiple pairwise post hoc comparisons dissected expression across the brain regions, for either *TRPC3b* or *TRPC3c* transcript levels (Table 2; Fig. 2). These data show that the cerebellum had significantly greater *TRPC3* expression than the other brain regions and that only this region exhibited *TRPC3c* transcript abundance that approached *TRPC3b* levels.

**Table 2** Statistical summary of expression levels of *TRPC3b* and *TRPC3c* normalised to the reference genes, *β-ACTIN* and *GAPDH* (combined), for the seven brain regions shown in Fig. 2. *n.s.*, not significant; $p > 0.05$. Table entries are *p*-values for the indicated comparisons

| Brain region | Pons | Medulla | Cerebellum | Midbrain inferior |
|---|---|---|---|---|
| *TRPC3b* | | | | |
| Motor cortex | < 0.001 | < 0.001 | < 0.001 | n.s. |
| Hippocampus | 0.013 | < 0.001 | < 0.001 | n.s. |
| Midbrain superior | 0.002 | 0.008 | 0.005 | n.s. |
| Midbrain inferior | 0.007 | < 0.001 | < 0.001 | n.s. |
| Pons | – | < 0.001 | < 0.001 | n.s. |
| *TRPC3c* | | | | |
| Motor cortex | < 0.001 | n.s. | 0.004 | 0.026 |
| Hippocampus | 0.032 | 0.026 | < 0.001 | n.s. |
| Midbrain superior | n.s. | 0.039 | 0.002 | n.s. |
| Midbrain inferior | n.s. | < 0.001 | < 0.001 | n.s. |
| Pons | – | < 0.001 | < 0.001 | n.s. |

The *TRPC3b* transcript number was typically ~ 1/200th of either of the reference genes in all brain regions except the pons, where it was lower (~ 1/1000th), and in the medulla and cerebellum, where it was higher (~ 1/50th of *β-ACTIN* and *GAPDH* transcript copy number, Fig. 2 a, b; Table 2; Supplementary Table 7; with Supplementary Fig. 6 providing data on an individual basis). In comparison, the *TRPC3c* transcript abundance in motor cortex, hippocampus and medulla was ~ 10 times lower than *TRPC3b*. This increased to a 1000 times differential in the midbrain (superior and inferior) and pons. In contrast, in the cerebellum, the normalised *TRPC3c* transcript copy numbers approached one-fourth of the *TRPC3b* copy number (Fig. 2 a, b; Table 2; Supplementary Table 7; with Supplementary Fig. 6 providing data on an individual basis). The greatest variation within a region, for the *TRPC3b* transcript, was within the medulla and cerebellum, with limited variance in the other brain regions (Fig. 2 a, b; Supplementary Fig. 6; Supplementary Table 7). In contrast, the variance was broader across all brain regions for the *TRPC3c* transcript (Fig. 2 a, b; Supplementary Fig. 6; Supplementary Table 7).

### Proportional Comparison of *TRPC3b* and *TRPC3c* mRNA Transcript Levels Across Brain Regions

The mean proportions of the two *TRPC3* splice variant transcript levels (*TRPC3c* copy number/*TRPC3b* copy number) for each tissue sample provided a direct comparison of expression levels of the two isoforms for individual brain regions (Fig. 3; Table 3). *TRPC3c*/*TRPC3b* proportions were in the range of 0.04–0.09 (~ 1/25th–1/10th) across all brain regions except for the cerebellum, which had *TRPC3c* transcript levels ~ 2.5 times more abundant (0.251 ± 0.049) than the next highest region (medulla) and exhibited the largest variability (range 0.05 to 0.48). The absolute copy numbers of the *TRPC3b* and *TRPC3c* mRNA transcripts varied considerably in the cerebellum (range 986–66,350 for *TRPC3b*; 132–29,386 for *TRPC3c*, where this variance was not correlated with differences in individual abundance of the reference gene copy numbers; Supplementary Tables 3, 4, 5, and 6; Supplementary Fig. 4). One sample *t* tests determined that the proportions differed from unity (equal expression) in all brain regions, indicating the dominance of the TRPC3b isoform (Table 3). Ranked two-way ANOVA determined that the increased expression of the TRPC3c isoform in the cerebellum was significantly greater than the pons and midbrain using this approach ($p = 0.011$, $p = 0.015$, respectively); otherwise, the regions did not differ significantly ($p > 0.05$).

## Discussion

Messenger RNA transcript levels for the *TRPC3b* and *TRPC3c* splice variants varied across seven different brain regions examined in tissue from human subjects. The cerebellum showed the most abundant expression of either isoform, and pons the weakest. The full-length *TRPC3b* mRNA transcript was the most abundant in all regions, both in terms of

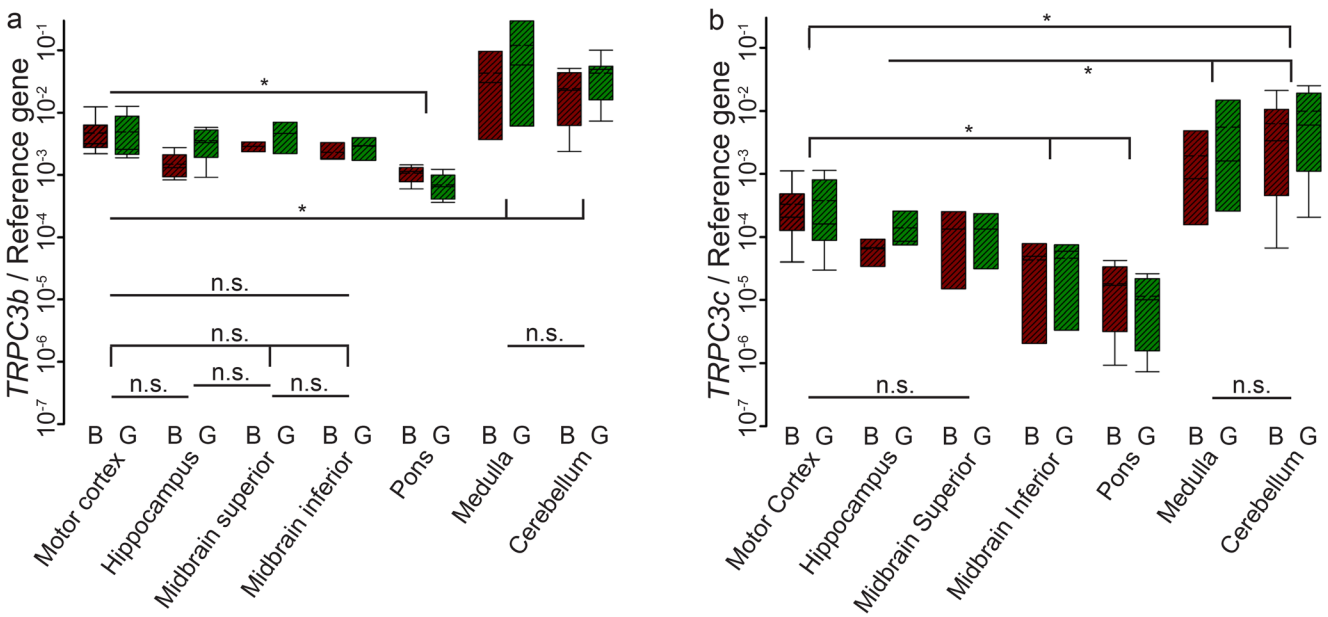


**Fig. 2** *TRPC3b* (**a**) and *TRPC3c* (**b**) mean expression levels normalised to each reference gene, *β-ACTIN* (B) and *GAPDH* (G), for each of the seven brain regions. The mean expression level of *TRPC3b* and *TRPC3c* is highest in the cerebellum and the medulla, with no significant difference between the two brain regions. There is no significant difference between the data on *TRPC3b* and *TRPC3c* copy number normalised to either of the reference genes ($p = 0.172$, three-way ANOVA). n.s., not significant ($p > 0.05$). Median, solid line and mean, dashed line. *$p < 0.05$. See Table 2 for a statistical summary

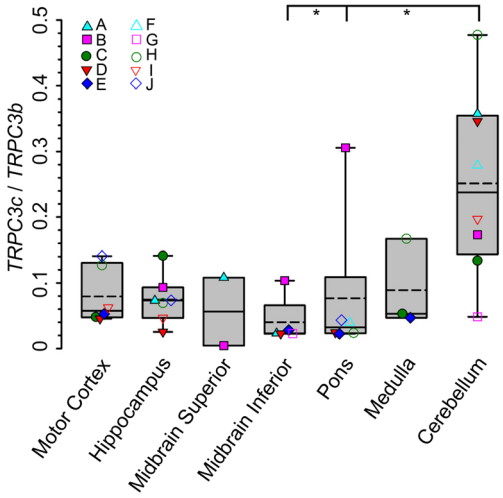


**Fig. 3** Boxplot of *TRPC3c/TRPC3b* proportions in seven brain regions from 10 human subjects (A, filled cyan upward triangle; B, filled pink square; C, filled green circle; D, filled red downward triangle; E, filled blue diamond; F, open cyan upward triangle; G, open pink square; H, open green circle; I, open red downward triangle; J, open blue diamond). The highest relative expression was found in the cerebellum (0.251 ± 0.05), with the lowest relative expression in the inferior midbrain (0.04 ± 0.02). The relative proportion of *TRPC3c* was significantly higher in the cerebellum compared to the relative proportion in pons (*$p = 0.011$) and midbrain inferior (*$p = 0.015$). However, *TRPC3b* was the dominant splice variant in all brain regions (one sample *t* test). See Table 3 for a statistical summary

**Table 3** *TRPC3c/TRPC3b* mean proportions ± SEM in seven brain regions for the human subjects (A-J) shown in Fig. 3. The relative proportion of *TRPC3c* is significantly more expressed in the cerebellum compared to the other six brain regions However, *TRPC3b* is the dominant isoform in all brain regions (one sample *t* test; ^ = ranked)

| Brain region | Mean proportion (*TRPC3c/TRPC3b*) | SEM | One sample *t* test |
|---|---|---|---|
| Motor cortex^ | 0.079 | 0.018 | $p = 0.022$ |
| Hippocampus | 0.075 | 0.014 | $p < 0.001$ |
| Midbrain superior | 0.057 | 0.052 | $p = 0.035$ |
| Midbrain inferior^ | 0.04 | 0.016 | $p = 0.047$ |
| Pons^ | 0.077 | 0.046 | $p = 0.022$ |
| Medulla | 0.089 | 0.039 | $p = 0.002$ |
| Cerebellum | 0.251 | 0.049 | $p < 0.001$ |

relative copy number and proportional analysis. Based on the latter, the truncated TRPC3c isoform approached 25% of the TRPC3b abundance in the cerebellum (1 copy of TPRC3c for every 3 copies of TRPC3b). This level of *TRPC3c* expression is qualitatively less than what has been reported previously for the cerebellum in other species, where *TRPC3c* is equivalent in abundance (guinea pig) or dominant (mouse and rat) [14]. However, we noted that the proportional representation of *TRPC3c* relative to *TRPC3b* in the cerebellum had higher variance than other brain regions, with one subject reaching 0.48. In addition, the absolute *TRPC3b* and *TRPC3c* mRNA transcript copy numbers varied greatly (a factor of 67 in range for *TRPC3b* and a factor of 222 for *TRPC3c*; Supplementary Tables 3 and 4, Supplementary Fig. 4). The Kim et al. study [14], indicated that the lowest level of *TRPC3c* mRNA transcript relative to *TRPC3b* was found in the cerebral cortex for all three animal species, while the present study showed that lowest ratio of *TRPC3c*: *TRPC3b* was in the midbrain. Maintenance of the relatively abundant level of the TRPC3c isoform in the human cerebellum, albeit at a proportionately lower level relative to TRPC3b than seen in rodents (mouse = rat, > guinea pig), may reflect selection against the greater conductance and associated $Ca^{2+}$ entry of the (truncated) TRPC3c isoform in the Purkinje neurons [14] in longer living species.

Given that TRPC3 ion channels assemble as tetramers [24] and in the cerebellum TRPC3 homomers are known to be the dominant type of TRPC channels, particularly in the mouse Purkinje neurons [3, 24], then the current finding of a 1:3 transcript ratio for *TRPC3c*: *TRPC3b* suggests likely modification of the properties of the TRPC3 channels by integration of TRPC3c subunits in the cerebellum compared with these channels in other brain regions. Comparison of heterologously expressed TRPC3c channels with TRPC3b channels (mouse isoform) indicate an increased channel conductance and associated higher $Ca^{2+}$ influx compared with the full-length isoform [15]. This has been validated with targeted mutations around the C-terminal region affected by the loss of intron 9 in the TRPC3c isoform [25].

The abundance of *TRPC3* mRNA of both isoforms in the cerebellum is entirely consistent with in situ hybridization studies in mouse [6, 24], which shows that the cerebellum and olfactory bulb have the highest signal levels. *TRPC3* mRNA signal is also abundant in the hippocampus dentate gyrus region and at a lesser level in the cerebral cortex. These studies do not discriminate between TRPC3b and TRPC3c isoforms. Equivalent mRNA localization studies have not been undertaken on human tissue. Similarly, quantitative analysis of *TRPC3* transcript levels in individual mouse Purkinje neurons demonstrates a 6 times great level of expression over the next most abundant transcript (*Trpc1*) [24]. TRPC3 subunits can co-assemble with TRPC6 and TRPC7 subunits in vitro [7, 26] and in vivo [27]. More recently, TRPC3 has also been shown to form heteromers with TRPC1 and/or TRPC4 [28, 29].

Further evidence that in the (mouse) cerebellar Purkinje neurons, TRPC3 ion channels are homomeric stems from electrophysiological data. The TRPC3 channels are non-selective cation channels coupled to the mGluR that underlie the slow excitatory post-synaptic current (sEPSC) with activation of the parallel fibre input pathway or direct pharmacological activation with the mGluR1 agonist (S)-3,5-dihydroxyphenylglycine (DHPG) [3]. This sEPSC is absent in mice null for *Trpc3* [3].

While in the current study, we have been able to show brain region-specific expression of two TRPC3 isoforms; the analysis

of mRNA extracted from brain tissue blocks makes an inference of the underlying cell types expressing the *TRPC3* transcripts indeterminate. The post-mortem brain samples that we have analysed for *TRPC3* expression are a mix of neurons, glia and microvascular elements. Apart from expression in Purkinje neurons [3, 4, 24, 30], in situ hybridization experiments have shown that *Trpc3* is also expressed in unipolar brush cells (UBC) in adult mouse cerebellum [30]. These cells are localised in the granular layer in the vestibulocerebellum and only the type II UBCs express *Trpc3*. Interestingly, in contrast to the type I UBCs, the type II UBCs also express the mGluR1α, PLC β4 and DAG kinase β [31]. TRPC3 is also expressed in the vascular endothelium [28, 29, 32–34], in astrocytes [35] (as is TRPC 1, 2, 4 and 6; reviewed by [36]) and microglia (reviewed by [37]). Oligodendrocytes also express TRPC channels [38], but this is an area of less exploration compared to that of TRPC channels in astrocytes. G protein-coupled receptor activation of TRPC3 channels in cultured astrocytes leads to $Ca^{2+}$ loading and apoptotic signalling [39], further supporting the concept that dysregulation of these ion channels is a contributor to brain injury. This is supported by an oxygen–glucose deprivation model showing that pro-apoptotic Bcl-2 signalling was reduced in astrocytes from *Trpc3/6/7* knockout mice compared with wild-type controls [35]. These *Trpc3/6/7* null mice also had significantly reduced infarcts following cerebral ischaemia and reperfusion arising from middle cerebral artery occlusion (MCAO). Currently, there is no information about alternative splicing of *TRPC3* mRNA with regard to any specific cell type in the brain.

A recent study using the photothrombotic infarct stroke model showed heightened expansion of brain injury in the hours and days following focal ischaemic brain injuries directed to the cerebellar cortex compared with cerebral cortex in the same mice [16]. This finding may well be reconciled with the differentially greater expression of TRPC3 channels and, in particular, the influence of TRPC3c-based enhanced $Ca^{2+}$ loading into the cerebellar Purkinje neurons, compared with the cerebral cortex neurons (mediated by intrinsic coupling to the mGluR). The confirmation of pronounced TRPC3 expression in the human cerebellar cortex here and the validation of alternative splicing of *TRPC3* to produce a proportionately higher level of TRPC3c isoform in this tissue offers further support for this pathway as a significant mediator of posterior circulation stroke in humans. The high variance in *TRPC3b* and *TRPC3c* expression in the cerebellum across individuals, as discussed above, may also indicate that some people may be at greater risk than others to stressor-induced cerebellar pathology.

## Conclusion

Expression of two functionally distinct isoforms of the TRPC3 non-selective cation channel varies significantly across brain regions in humans. The highest abundance of both isoforms is found in the cerebellum and in this region, the proportion of the high-conductance TRPC3c isoform is greater than in the other brain regions examined, albeit with maintained dominance of the unspliced TRPC3b isoform. The contribution of both these isoforms to glutamatergic neuromodulation via coupling to the metabotropic glutamate receptor lends the possibility that in pathological states, this signalling cascade contributes to focal ischaemic brain injury, particularly in the cerebellum.

**Funding information** This study was funded by the University of New South Wales Faculty Goldstar awards.

## Compliance with Ethical Standards

The Sydney Brain Bank (Neuroscience Research Australia) and the New South Wales (NSW) Tissue Resources Centre (Department of Pathology, University of Sydney), where the human tissues were obtained, have approvals from relevant human research ethics committees. Tissue requests are reviewed and approved by the NSW Brain Banks Scientific Review Committee or the National Institutes of Health (NIAAA) Scientific Advisory Board. The study was approved by the UNSW Sydney Human Research Ethics Committee.

**Conflict of Interest** The authors declare that they have no conflict of interest.

## References

1. Riccio A, Medhurst AD, Mattei C, Kelsell RE, Calver AR, Randall AD, et al. mRNA distribution analysis of human TRPC family in CNS and peripheral tissues. Brain Res Mol Brain Res. 2002;109(1–2):95–104.
2. Chung YH, Sun Ahn H, Kim D, Hoon Shin D, Su Kim S, Yong Kim K, et al. Immunohistochemical study on the distribution of TRPC channels in the rat hippocampus. Brain Res. 2006;1085(1):132–7.
3. Hartmann J, Dragicevic E, Adelsberger H, Henning HA, Sumser M, Abramowitz J, et al. TRPC3 channels are required for synaptic transmission and motor coordination. Neuron. 2008;59(3):392–8.
4. Huang WC, Young JS, Glitsch MD. Changes in TRPC channel expression during postnatal development of cerebellar neurons. Cell Calcium. 2007;42(1):1–10.
5. Ding SL, Royall JJ, Sunkin SM, Ng L, Facer BA, Lesnar P, et al. Comprehensive cellular-resolution atlas of the adult human brain. J Comp Neurol. 2016;524(16):3127–481.
6. © 2010 Allen Institute for Brain Science. Allen Human Brain Atlas. Available from: human.brain-map.org.
7. Hofmann T, Schaefer M, Schultz G, Gudermann T. Subunit composition of mammalian transient receptor potential channels in living cells. Proc Natl Acad Sci U S A. 2002;99(11):7461–6.
8. Birnbaumer L. The TRPC class of ion channels: a critical review of their roles in slow, sustained increases in intracellular $Ca^{(2+)}$ concentrations. Annu Rev Pharmacol Toxicol. 2009;49:395–426.
9. Kiselyov K, Xu X, Mozhayeva G, Kuo T, Pessah I, Mignery G, et al. Functional interaction between InsP3 receptors and store-operated Htrp3 channels. Nature. 1998;396(6710):478–82.

10. Vazquez G, Wedel BJ, Trebak M, St John Bird G, Putney JW Jr. Expression level of the canonical transient receptor potential 3 (TRPC3) channel determines its mechanism of activation. J Biol Chem. 2003;278(24):21649–54.
11. Yuan JP, Zeng W, Huang GN, Worley PF, Muallem S. STIM1 heteromultimerizes TRPC channels to determine their function as store-operated channels. Nat Cell Biol. 2007;9(6):636–45.
12. Zeng W, Yuan JP, Kim MS, Choi YJ, Huang GN, Worley PF, et al. STIM1 gates TRPC channels, but not Orai1, by electrostatic interaction. Mol Cell. 2008;32(3):439–48.
13. Tang J, Lin Y, Zhang Z, Tikunova S, Birnbaumer L, Zhu MX. Identification of common binding sites for calmodulin and inositol 1,4,5-trisphosphate receptors on the carboxyl termini of trp channels. J Biol Chem. 2001;276(24):21303–10.
14. Kim Y, Wong AC, Power JM, Tadros SF, Klugmann M, Moorhouse AJ, et al. Alternative splicing of the TRPC3 ion channel calmodulin/IP3 receptor-binding domain in the hindbrain enhances cation flux. J Neurosci. 2012;32(33):11414–23.
15. Kim YS, Housley GD. Homo sapiens transient receptor potential cation channel subfamily C member 3 variant c (TRPC3) mRNA, partial cds, alternatively spliced. GenBank; 2013.
16. Gorlamandala N, Parmar J, Craig AJ, Power JM, Moorhouse AJ, Krishnan AV, et al. Focal ischaemic infarcts expand faster in cerebellar cortex than cerebral cortex in a mouse photothrombotic stroke model. Transl Stroke Res. 2018;9:643–53.
17. Xu XZ, Li HS, Guggino WB, Montell C. Coassembly of TRP and TRPL Produces a Distinct Store-Operated Conductance. Cell. 1997;89(7):1155–64.
18. Greenwood D, Jagger DJ, Huang L-C, Hoya N, Thorne PR, Wildman SS, et al. P2X receptor signaling inhibits BDNF-mediated spiral ganglion neuron development in the neonatal rat cochlea. Development. 2007; 134(7):1407–17.
19. Mori R, Wang Q, Danenberg KD, Pinski JK, Danenberg PV. Both β-actin and GAPDH are useful reference genes for normalization of quantitative RT-PCR in human FFPE tissue samples of prostate cancer. The Prostate. 2008; 68(14):1555–60.
20. Ginzinger DG. Gene quantification using real-time quantitative PCR: an emerging technology hits the mainstream. Exp Hematol. 2002;30(6):503–12.
21. Pfaffl MW, Georgieva TM, Georgiev IP, Ontsouka E, Hageleit M, Blum JW. Real-time RT-PCR quantification of insulin-like growth factor (IGF)-1, IGF-1 receptor, IGF-2, IGF-2 receptor, insulin receptor, growth hormone receptor, IGF-binding proteins 1, 2 and 3 in the bovine species. Domest Anim Endocrinol. 2002;22(2):91–102.
22. Karge WH 3rd, Schaefer EJ, Ordovas JM. Quantification of mRNA by polymerase chain reaction (PCR) using an internal standard and a nonradioactive detection method. Methods Mol Biol. 1998;110: 43–61.
23. Weickert CS, Sheedy D, Rothmond DA, Dedova I, Fung S, Garrick T, et al. Selection of reference gene expression in a schizophrenia brain cohort. Aust N Z J Psychiatry. 2010;44(1):59–70.
24. Hartmann J, Konnerth A. TRPC3-dependent synaptic transmission in central mammalian neurons. J Mol Med (Berl). 2015;93(9):983–9.
25. Sierra-Valdez F, Azumaya CM, Romero LO, Nakagawa T, Cordero-Morales JF. Structure-function analyses of the ion channel TRPC3 reveal that its cytoplasmic domain allosterically modulates channel gating. J Biol Chem. 2018;293(41):16102–14.
26. Strubing C, Krapivinsky G, Krapivinsky L, Clapham DE. Formation of novel TRPC channels by complex subunit interactions in embryonic brain. J Biol Chem. 2003;278(40):39014–9.
27. Goel M, Sinkins WG, Schilling WP. Selective association of TRPC channel subunits in rat brain synaptosomes. J Biol Chem. 2002;277(50):48303–10.
28. Lichtenegger M, Groschner K. TRPC3: A Multifunctional Signaling Molecule. In: Nilius B, Flockerzi V, editors. Handbook of experimental pharmacology 222 mammalian transient receptor potential (TRP) cation channels. 1. Berlin Heidelberg: Springer-Verlag; 2014. p. 67–84.
29. Poteser M, Graziani A, Rosker C, Eder P, Derler I, Kahr H, et al. TRPC3 and TRPC4 associate to form a redox-sensitive cation channel. Evidence for expression of native TRPC3-TRPC4 heteromeric channels in endothelial cells. J Biol Chem. 2006;281(19):13588–95.
30. Sekerkova G, Kim JA, Nigro MJ, Becker EB, Hartmann J, Birnbaumer L, et al. Early onset of ataxia in moonwalker mice is accompanied by complete ablation of type II unipolar brush cells and Purkinje cell dysfunction. J Neurosci. 2013;33(50):19689–94.
31. Sekerkova G, Watanabe M, Martina M, Mugnaini E. Differential distribution of phospholipase C beta isoforms and diaglycerol kinase-beta in rodents cerebella corroborates the division of unipolar brush cells into two major subtypes. Brain Struct Funct. 2014;219(2):719–49.
32. Senadheera S, Kim Y, Grayson TH, Toemoe S, Kochukov MY, Abramowitz J, et al. Transient receptor potential canonical type 3 channels facilitate endothelium-derived hyperpolarization-mediated resistance artery vasodilator activity. Cardiovasc Res. 2012;95(4):439–47.
33. Di A, Malik AB. TRP channels and the control of vascular function. Curr Opin Pharmacol. 2010;10(2):127–32.
34. Earley S, Brayden JE. Transient receptor potential channels in the vasculature. Physiol Rev. 2015;95(2):645–90.
35. Chen X, Lu M, He X, Ma L, Birnbaumer L, Liao Y. TRPC3/6/7 knockdown protects the brain from cerebral ischemia injury via astrocyte apoptosis inhibition and effects on NF-small ka, CyrillicB Translocation. Mol Neurobiol. 2017;54(10):7555–66.
36. Cornillot M, Giacco V, Hamilton NB. The role of TRP channels in white matter function and ischaemia. Neurosci Lett. 2019;690:202–9.
37. Echeverry S, Rodriguez MJ, Torres YP. Transient receptor potential channels in microglia: roles in physiology and disease. Neurotox Res. 2016;30(3):467–78.
38. Marques S, Zeisel A, Codeluppi S, van Bruggen D, Mendanha Falcao A, Xiao L, et al. Oligodendrocyte heterogeneity in the mouse juvenile and adult central nervous system. Science. 2016;352(6291):1326–9.
39. Miyano K, Morioka N, Sugimoto T, Shiraishi S, Uezono Y, Nakata Y. Activation of the neurokinin-1 receptor in rat spinal astrocytes induces Ca2+ release from IP3-sensitive $Ca^{2+}$ stores and extracellular $Ca^{2+}$ influx through TRPC3. Neurochem Int. 2010;57(8):923–34.